aniel.thompson@nrcan-rncan.gc.ca]DanThompson

Incorporating fire severity for refined data-drive carbon emissions estimates of boreal and temperate forest fires in the Carbon Budget Model for Canadian forests

[1], [d[1], Ellen Whitman[2], Hafer Mark[3], Oleksandra Hararuk[2], Chelene Hanes[1], Vinicius Manvailer Goncalves[3], and Ben Hudson[3]

[1]Natural Resources Canada, Canadian Forest Service, Great Lakes Forestry Centre, Sault Ste. Marie, Canada
[2]Natural Resources Canada, Canadian Forest Service, Northern Forestry Centre, Edmonton, Canada
[3]Natural Resources Canada, Canadian Forest Service, Pacific Forestry Centre, Victoria, Canada

Correspondence: Dan Thompson (daniel.thompson@nrcan-rncan.gc.ca)

Abstract. Wildfire is the most impactful natural disturbance to Canada's boreal and temperate forest biomes. Current representations of fire impact on forest carbon stocks is limited to a single parameterization of fire severity (i.e. the fraction of biomass consumed) that assumes only high severity fires, despite a large and increasing evidence base of widespread mixed-severity wildfire. In this submodel of the larger Generic Carbon Budget Model for forest carbon accounting, field measurements of biomass consumption as related to satellite-derived burn severity maps are interpretted from a fire physics and ecology perspective to derive algorithms to describe forest carbon fluxes in the immediate aftermath of fires. Model outputs indicate total carbon emissions range from a 11 t C/ha in Boreal Shield West forests of Saskatchewan following low severity fire to over 70 t C/ha in Taiga Cordillera and Pacific Maritime forests of Yukon under high severity fire. Pacific Maritime forest showed the largest fraction of carbon release in the canopy biomass pools (67%), while Taiga Shield West and Boreal Plains of the Northwest Territories and Manitoba were estimated of having 82% of carbon emissions in the surface and organic soil biomass pools of litter, duff, and roots

1 Introduction

Wildfire is on par with insects as the largest stand-replacing disturbance process in Canada's forest, impacting ~1-3 Mha of Canada's 355 Mha forested area in a typical year (Hanes et al., 2019). In Canada's reliable 53-year burned area record, nine years have exceeded 4 Mha of burned area (or approximately 1% of Canada's forest area) (Skakun et al., 2022). The 2023 fire season in Canada burned a remarkable 15 Mha owing to extreme drought, severe fire weather conditions, and a prolonged fire season length (Jain et al., 2024).

Of this, publicly-owned managed forest under long or short-term tenure accounts for 23% of the area burned between 1972 and 2024; publicly-owned managed forest under long-term licence to private timber companies forms 40% of Canada's forest area (Stinson et al., 2019). Privately-owned forest constitutes only 6% of the forest area (and 0.5% of area burned), with the remainder of the forest area being a mix of formally protected areas, remote unmanaged forest, Indigenous reserve lands and other uses without large-scale harvesting. Managed forest areas adjacent to communities have historically shown some meaningful local fire suppression effects with a bias towards older forest nearby boreal forest communities in Canada, though the effect is limited to a 25 km radius between these widely dispersed communities (Parisien et al., 2020).

Burned area in Canada is dominated by a relatively small number of very large fires, with 3% of fires constituting 97% of the burned area (Stocks et al., 2002). Lightning-caused fires account for approximately half of all ignitions and approximately 80% of burned area, but no distinction is made between human and lightning ignition for carbon accounting purposes. Annual burned area mapping for carbon reporting in Canada is conducted using a composite of satellite and aerial mapping at 30 metre resolution; the relatively small number of large fires, and their slow vegetation regeneration (White et al., 2017) allows for reliable mapping using multi-spectral imagery such as Landsat within one year of the fire (Whitman et al., 2018).

[2 sentences on CBM-CFS3 and simple stuff about it]..... In CBM-CFS, spatially referenced stand lists representing large homogenous stands that fall within spatial units (ecozone-provincial intersections) (Kurz et al., 2002), even when applying precisely mapped burned areas (Hall et al., 2020). CBM-CFS currently assesses fire impacts to carbon pools only as representing high-severity fire, which is the most common of three severity classes of burned forest in Canada (Hall et al., 2008). Currently, biomass consumption estimates are based on the and the assumption of complete crown mortality, with additional biomass consumption following a spatially-referenced aggregated estimate at the ecozone-province of annualized drought conditions. Quantification of the change in carbon stock in CBM is made via a "Disturbance Matrix" (hereafter referred to as a DM) which is simply a matrix of the proportional mass flux of carbon between each pair of pools in the model for a site experiencing a given disturbance. This proportional mass flux is independent of the size of the C pool. Pools in the DM include all the above and below-ground pools tracked in CBM, as well as an atmospheric sink pool. Importantly, unlike an emissions-only fire models commonly used in air quality modelling in Canada (Chen et al., 2019), DM definitions in CBM also track the transfer of live biomass to dead, but still uncombusted pools such as live stemwood (which are killed but not burned) to standing deadwood, also known as snags.

In Canada's forests, a combination of disturbance history, soils, and less frequently topographic variables determine leading tree species; at local scales (1-100 ha), tree species plays a major role in determining ecosystem susceptibility to fire (Bernier et al., 2016) where older, conifer-dominated forests burn at very high rates relative to adjacent deciduous or mixed stands. Even when deciduous and mixed forests do burn, they do so at consistently lower severity compared to all but the most xeric conifer forests (Whitman et al., 2018). Thus, important local biases in fire activity towards older and moderate to poorly-drained forests are not resolved in the spatially-referenced CBM-CFS3 when only a regionally-averaged fire severity is applied.

To support recent advances in operational burn severity mapping for Canada (Whitman et al., 2020) alongside multi-decade reliable burned area records that provide certainty on fire start and end dates (Hall et al., 2020), this paper describes a local scale (30-m) method for defining a per-pixel proportional carbon flux measurement via a locally calculated fire DM. In this

document, we outline the evidence-based fire Disturbance Matrices updated and designed for a spatially-explicit update to the CBM, anchored in a three severity class paradigm. These fire carbon flux models are built from a blend of aggregated field data linked to remotely sensed severity, as well as insights from fire physics and experimental fires. Key knowledge gaps are also highlighted, with interim solutions presented until further quantification can be done in field studies, such as from further wildfire observations, experimental fires, or prescribed fires.

Simplified fire DMs (i.e. a scalar reduction on 100% mortality assumption) have been used in scenario exercises using CBM for assessment of future fire and harvest scenarios (Smyth et al., 2022); the algorithm development shown here provides an important data-driven and regionally-adjusted framework that better reflects the ecological nuances of moderate and low-severity fire across Canada's diverse ecozones.

2 Methods

2.1 Carbon Modelling

2.2 Carbon Modelling Spatial Units

2.3 Biomass pools of the Generic Carbon Budget Model

Short section explaining the pool definitions most relevant to fire.

2.4 Axioms of forest carbon budget after fire

To simplify the process of the creation of the DMs as a distillation of the complexities of fire severity and combustion patterns, the following logical axioms are proposed and maintained throughout:

1. Disturbance matrices are to be in terms of mortality, not survival. Mortality here is defined as tree death by the end of the calendar year of the fire's occurrence. Tree mortality in subsequent years is not modelled here.
2. Crown Fraction Burned (CFB) is a mass-based estimate of the portion of foliage consumed in the flaming passage of a fire, and is inclusive of merchantable and submerchantable trees, both broadleaf and needleleaf. Needles that are heat-killed but otherwise not consumed in the fire are not considered part of CFB, and are instead considered part of the foliage to litter biomass transfer.
3. The heat-killed but unconsumed fraction of the canopy is equal to (mortality - CFB).
4. In submerchantable trees, mortality == CFB.
5. In merchantable trees, CFB <= mortality.
6. Snags are inclusive of both those killed by prior fire as well as those killed by all other causes.

Table 1. Emissions factors in flaming and smouldering phase, expressed as portion of unburned biomass carbon content

Spp	Flaming	Smouldering
CO2	0.868	0.703
CO	0.070	0.161
PM10	0.022	0.048
NMOG	0.016	0.035
PM25	0.019	0.040
CH4	0.005	0.013
BC	0.000	0.000

Of these, Crown Fraction Burned (CFB) is an important concept used primarily in fire behaviour science but not carbon accounting nor fire ecology. CFB was introduced in the 1992 Fire Behaviour Prediction System documentation (Group, 1992), and provides a simple continuous 0-100 variable for only the consumption of foliage (inclusive of both conifer and broadleaf). For our purposes, CFB is the desirable metric as opposed to ordinal and less precise systems like Canopy Fire Severity Index (Kasischke et al., 2000) that allows the user to specify which pools of canopy biomass are consumed, but not the precise fraction of each given pool that is consumed.

2.5 Ground plot and remotely sensed fire severity data

!!!Ellen to insert methods here - including the figure of where the samples are from etc.

2.6 Combustion gas emission ratios

Certain variables, like the partitioning of CO_2:CH_4:CO gas emissions, are constant throughout ecozones, but vary by flaming vs smouldering combustion modes. The precise emissions ratios vary slightly between models and field studies, but for this initial algorithm assessment, we define these emissions ratios as being identical to those used in Canada's operational wildfire smoke forecasting system, FireWork (Chen et al., 2019). They are defined in a global variables table:

where CO_2 is responsible for 86.8% of emissions in the flaming phase, but only 70.3% of emissions in the smouldering phase, with a doubling of CO emissions and tripling of CH_4 emissions. With a Global Warming Potential of CO equal to 1.9 and CH_4 of 25, the Global Warming Potential per unit of biomass consumption in the smouldering phase is 1.18 times higher in global warming potential compared to flaming, not including differential aerosol production and injection heights, however. With flaming and smouldering each contributing roughly equally to wildfire emissions, these distinct flaming and smouldering emissions ratios correspond well prior emissions factors used in CBM. Note that as current described, the sum of CO_2, CH_4, and CO emissions from wildfires only represent approximately 95% of the fire carbon mass emitted to the atmosphere, with 0.5-2.0% of biomass emitted as particulate matter (e.g. PM2.5, but also PM1 and PM10 classes of particulates at 1 and 10

Table 2. Unburned litter area by ecozone and severity class. The majority of the data comes from studies in the Boreal Plains and Boreal Shield West, and so values are extrapolated from those two well-observed ecozones to all others.

Ecozone	Low	Mod	High
BSW	0.20	0.08	0.05
TP	0.14	0.16	0.03
TSW	0.20	0.08	0.05
BP	0.14	0.06	0.02
BC	0.14	0.06	0.02
BSE	0.20	0.08	0.05
TSE	0.20	0.08	0.05
MC	0.14	0.06	0.02
HP	0.20	0.08	0.05
TC	0.14	0.06	0.02
PM	0.14	0.06	0.02
AM	0.14	0.06	0.02
MP	0.14	0.06	0.02
P	0.14	0.06	0.02

um diameters, respectively), and an additional 3% (Hayden et al., 2022) to as little as 1% (Simon et al., 2010) composed of non-methane organic gases that have a large range in global warming potentials as compared to CH_4.

2.7 Litter layer area-wise consumption by severity class

The litter layer forms the first biomass pool in which a spreading fire consumes fuel. In low-severity fires, the litter layer may be consumed little to no underlying duff material consumed, nor any tree mortality (Hessburg et al., 2019). Logically, since litter consumption is largely required for the ignition of the underlying duff layer, this litter area-wise fractional consumption also informs and constrains duff consumption.

2.8 Forest Floor Consumption

While consumption of fine fuels in the litter layer of the forest floor is nearly complete for any given fire intensity, consumption of deeper organic soil horizons (F+H layers in upland forests and upper peat layers in wetlands) is more drought dependent. In the fire literature in Canada, the soil organic layer is sometimes termed the Forest Floor Fuel Load (*FFFL*) (Letang and de Groot, 2012) and is dominated by the equivalent organic soil Slow pool (Aboveground Slow Dead Organic Matter, or AGSlowDOM) in CBM. Typically attention has been paid to the absolute value of Forest Floor Fuel Consumption (*FFFC*); however in the case of carbon modelling, it is the relative fraction of consumption (*FFFC/FFFL*) that is of interest. In this

scheme, we utilize a composite of wildfire data from (de Groot et al., 2009) alongside the ABoVE duff consumption data (Walker et al., 2020), with an alternative modelling approach to compute the relative amount of depth of consumption (scalar from 0 to 1) rather than an absolute value in kg m^{-2} or cm as otherwise done in the literature. A logit transform is used on the scalar data to make it suitable for the fitted non-linear least-squares modelling:

$$logit\left(\frac{depthofburn}{prefiredepth}\right) = [3.83(1 - e^{(-0.005DC)})] + (-0.718log_e(AGSlow)) \quad (1)$$

where DC is the Fire Weather Index Drought Code, and AGSlow in the CBM (given in Mg C/ha in this equation), and also synonymous with the the Forest Floor Fuel Load (with ecozone averages given in (Letang and de Groot, 2012) or site-level data where observed). The modelling of relative depth of burn had a higher skill than modelling of the relative mass of consumption, given natural variability in soil density with depth.

A conversion factor is then applied to the relative depth of burn data to convert it to a relative mass consumption value. Since organic soil density always increases non-linearly with depth, this conversion factor from depth to mass is less than one:

$$\left(\frac{massconsumed}{prefiremass}\right) = \left(\frac{depthofburn}{prefiredepth}\right) * CF \quad (2)$$

where the Correction Factor is defined for boreal spruce fuel types as:

$$CF_{spruce} = 1.018(RelativeDepth)^{0.250} \quad (3)$$

and for all other fuels as

$$CF_{nonspruce} = 0.13(RelativeDepth) + 0.87 \quad (4)$$

with RelativeDepth as a value from 0-1.

While ultimately this scheme can be used on individual fires with estimated or measured fuel loading and specific Drought Code values, for the purposes of this first assessment, an ecozone-averaged fuel load and decadal composites of Drought Code can also be used to provide representative values. Specifically, a median Drought Code of detected fire hotspots in Canada from 2003-2021 (Barber et al., 2024) using the same data as the Canadian CFEEPS-FireWork wildfire air quality model of (Chen et al., 2019) is presented below, along with proportional consumption values of the forest floor by ecozone:

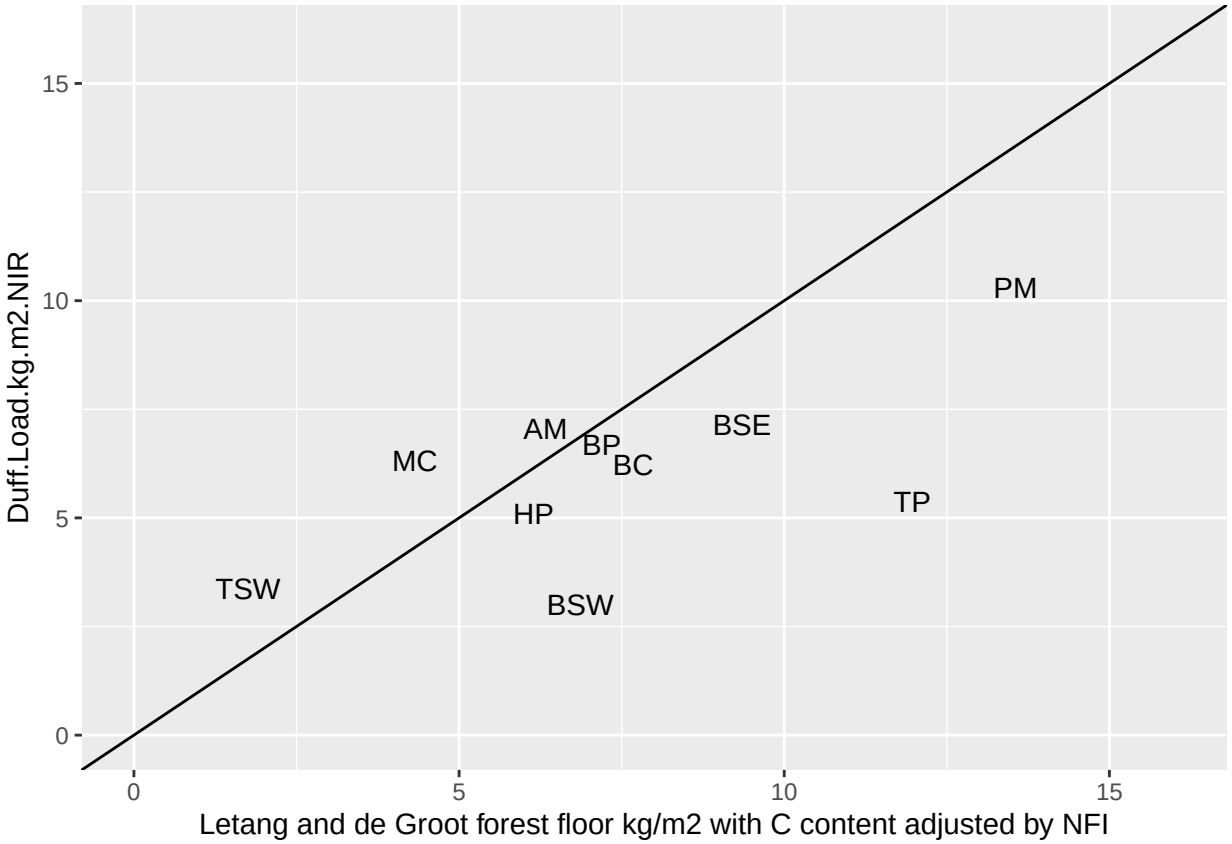

Note that the maximum upland Forest Floor Fuel Load is approximately 30 kg m-2 (150 Mg C/ha) (Letang and de Groot, 2012); higher values are typically seen only in peat ecosystems, where the above scheme is less representative at a local scale since the fuel load (pool size) in peatlands is much larger, but absolute consumption values are similar between deep forest floor organic layers and peatlands (Walker et al., 2020). For Canadian peatlands, the CaMP model (Bona et al., 2020) is instead used in CBM. Within CaMP, a separate peatland water model driven by Drought Code determines the thickness of the unsaturated peat layer, and an amount approximating 12% of the thickness of the unsaturated peat is consumed as smouldering consumption. The peat-specific carbon pools and fire Disturbance Matrices are fully described in (Bona et al., 2020); large peatland trees will still utilize the DM scheme described below. Since deeper forest organic soil and peat layers show approximately similar absolute consumption rates, for the purpose of this general model description no peatland-specific components of the fire DMs are required.

Limited data is available on the fraction of woody debris consumption alongside fire severity measurements. Coarse woody debris of overstory stems that makes up 60-80% of woody debris biomass in Canada's boreal and temperate forests (Hanes et al., 2021), with its moisture and consumption patterns largely follows the moisture regime of the Drought Code (McAlpine, 1995). In this modelling framework, the proportion of coarse (>7.5 cm diameter) and medium (>0.5 cm and <7.5 cm) woody debris consumption is estimated based on detailed measurements of consumption from experimental fires. Coarse Woody

Table 3. Fire Weather, fuel loading, and duff consumption values per ecozone. Note that FFFL values are from Letang et al., (2012) and not directly from the Reporting Unit values provided in the National Inventory Report. Median Drought Code of burning is from Barber et al., (2024).

Ecozone	Median Drought Code of Burning	Median FFFL kg m-2	FFFC kg m-2	% consumption
BSW	239	6.864	3.22	0.47
TP	369	11.97	6.12	0.51
TSW	297	1.7556	1.37	0.78
BP	242	7.1932	3.34	0.46
BC	250	7.67844	3.56	0.46
BSE	123	9.3522	1.85	0.2
TSE	98	4.9764	1.15	0.23
MC	452	4.32	3.21	0.74
HP	204	6.1462	2.64	0.43
TC	254	7.7616	3.63	0.47
PM	268	13.5584	5.15	0.38
AM	270	6.33	3.35	0.53
MP	123	9.3522	1.85	0.2
P	242	7.1932	3.34	0.46

Debris is responsible for approximately 50-75% of the total woody debris load in most ecozones, and approximately 60% of the total woody debris consumption. Ecozone-level CWD consumption rates are summarized as:

Note that where historical burn severity data is not available, and instead the fire classification type of surface, intermittent crowning, and active crown fire are used as proxies for low, moderate, and high severity fire, respectively. Fine woody debris <0.5 cm in diameter is consumed at the exact same rate as the litter pool (see section above).

2.9 Drivers of C losses in the tree canopy

2.9.1 Overstory tree mortality and consumption

Numerous process-driven (Michaletz and Johnson, 2006) or empirical (Hood and Lutes, 2017) tree mortality models are present and show significant skill in predicting tree mortality based on fire behaviour (i.e. flame length, rate of spread). Since the driving data in this model is satellite-derived fire severity over the landscape scale, fire behaviour metrics such as flame length or scorching height of bark are not available as a continuous mapped product. Instead, softwood and hardwood overstory mortality is calculated per ecozone as a function of satellite-observed fire severity using aggregated ground plot data:

And since large-diameter, live trees killed by fire do not experience significant live stemwood consumption, the entirety of the live stemwood biomass pool that is killed is transferred to the snag pool. Note that the field data and disturbance modelling

Table 4. Coarse Woody debris consumption rates from pre/post measurements in experimental fires

Ecozone	Low	Mod	High
BSW	0.024	0.163	0.140
TP	0.000	0.218	0.238
TSW	0.000	0.218	0.238
BP	0.359	0.509	0.412
BC	0.024	0.163	0.140
BSE	0.080	0.131	0.182
TSE	0.080	0.131	0.182
MC	0.024	0.163	0.140
HP	0.080	0.131	0.182
TC	0.024	0.163	0.140
PM	0.024	0.163	0.140
AM	0.080	0.131	0.182
MP	0.080	0.131	0.182
P	0.359	0.509	0.412

Table 5. Softwood fractional mortality by ecozone, as dervied from median values from field studies

Ecozone	Low	Mod	High
BSW	0.45	0.81	1.00
TP	0.45	0.81	1.00
TSW	0.10	0.81	1.00
BP	0.45	0.81	1.00
BC	0.24	0.65	0.98
BSE	0.45	0.81	1.00
TSE	0.10	0.81	1.00
MC	0.28	0.74	0.98
HP	0.45	0.81	1.00
TC	0.24	0.65	0.98
PM	0.13	0.38	0.97
AM	0.28	0.34	0.95
MP	0.28	0.34	0.95
P	0.45	0.81	1.00

Table 6. Softwood crown fraction burned by ecozone, as dervied from median values from field studies

Ecozone	Low	Mod	High
BSW	0.0	0.81	1.00
TP	0.0	0.81	1.00
TSW	0.1	0.81	1.00
BP	0.0	0.81	1.00
BC	0.0	0.65	0.98
BSE	0.0	0.81	1.00
TSE	0.1	0.81	1.00
MC	0.0	0.74	1.00
HP	0.0	0.81	1.00
TC	0.0	0.65	1.00
PM	0.0	0.38	0.97
AM	0.0	0.34	0.95
MP	0.0	0.34	0.95
P	0.0	0.81	1.00

undertaken here only accounts for tree mortality within the calender year of the fire, and delayed mortality of over one year has been documented in boreal low and moderate severity fires (Angers et al., 2011)where less than half of total mortality occurs after the year of the fire. Thus, the modelling here does not account for delayed mortality that may extend upwards of 5 years after fire.

Crown Fraction Burned (CFB) speaks to the fraction of the live canopy that is itself consumed in the flaming front. The alternate outcomes being survival of the foliage, or the mortality of the tree without canopy consumption, resulting in the dropping of foliage onto the forest floor. From the axioms stated earlier, the CFB must be lower than or equal to the mortality rate, using field studies that show any partial crown consumption is likely sufficient to result in high rates if not complete mortality (Hood and Lutes, 2017), which is the case in Canada's trees with primarily thin bark. Due to the structure of the CBM, all High Severity fires have their mortality in the merchantable and smaller trees set to exactly 1.0, which is no more than a 5% variance from observed values. From field studies, the following ecozone-specific CFB values are found:

The consumption of live bark biomass is a pool in the model, and consumption rates can be defined by severity class. At the moment, lacking robust field data on bark biomass consumption rates across ecozones and severity classes (which are a small portion of the overall biomass), the bark proportional consumption rate is set to 34% of the overstory mortality rate, based only on a single set well-observed high severity fires in the Taiga Plains by [santín2015].

A major distinction is made between softwood and hardwood trees, where in Canada's boreal forests, a large fraction of hardwood trees (see Appendix E) are able to resprout even when the main stem has been killed by an intense forest fire (Brown

Table 7. Ecozone-level average fraction of hardwood overstory species that do not suffer extensive belowgroud biomass mortality after fire

Ecozone	Resprout Fraction
BSW	0.75
TP	0.75
TSW	0.94
BP	0.99
BC	0.76
BSE	0.67
TSE	0.78
MC	0.97
HP	0.80
TC	0.27
PM	0.39
AM	0.76
MP	0.32
P	0.99

and DeByle, 1987). Accordingly, the root mortality rates differ greatly between softwoods and hardwoods, with softwood root mortality equal precisely to stem mortality, while in resprouting hardwoods, little root mortality is observed even after intense fire (Pérez-Izquierdo et al., 2019). Though GCBM can resolve a species list down to the pixel level, currently an ecozone-level regional average composition of hardwood species with resprouting traits is used and is shown below:

Concurrently, the fraction of fine roots contained within the combustible forest floor layers can be a close to or exceeding 50% of the fine root biomass (Strong and La Roi, 1985), and burns alongside the organic soils (Benscoter et al., 2011). As a result, the calulation for softwood fine root consumption and mortality are as follows, using Softwood as an example:

$$SWFineRootConsump = SW.Mort \times SW.Prop.Fine.Root.duff \times Duff.Consump.Fract \tag{5}$$

$$\text{SWFineRootMort.AG} = \text{SW.Mort} \times SW.Prop.Fine.Root.duff \times (1 - Duff.Consump.Fract) \times (1 - ReSproutFactor)\text{SWFineRo}$$

In contrast, the larger diameter of the coarse root biomass pool prevents its consumption during any smouldering of the duff layer, and the mortality rate of coarse roots is simply proportional to that of the stemwood overall.

2.9.2 Understory tree mortality and consumption

Understory (or small diameter overstory) tree mortality is defined seperately in the model, but given the lack of data on diameter classes in the severity data, robust field data on differing mortality rates of smaller diameter trees is not available, and so the understory tree mortality rate is set equal to the overstory rate as defined in the table above. Note that trees with a top height less than 1.4 m are not considered in this pool, and instead are lumped into the "other" pool.

2.9.3 Snag and stump consumption

Dead standing trees and branches on average is a biomass pool much smaller than organic soils or coarse woody debris on the ground, but in areas of extensive insect killed trees, recent fires, and blowdown, is a substantial biomass pool. In this initial algorithm description, only typical boreal forest stands where snags are a small fraction of total stems are considered. Compared to live stemwood of the same diameter, the low moisture content of snags and snag branches allows for much greater consumption during the passage of an intense flaming front (Stocks et al., 2004). The snag branch pool experiences almost complete combustion in high severity fires (Talucci and Krawchuk, 2019), and is highly correlated with live foliage consumption (i.e Crown Fraction Burned) (de Groot et al., 2022). The largest biomass pool of the main standing dead stemwood remains at most approximately 50-60% consumed. In the absence of extensive field data from CBI plots to quantify snag and snag branch consumption, snag (dead stemwood) consumption fraction is estimated as:

$$SnagConsumptionfraction = (0.5 \times CrownFractionBurned) + 0.05 \tag{6}$$

And for snag branches:

$$SnagBranchConsumption = (0.9 \times CrownFractionBurned) \tag{7}$$

Stumps are tracked as their own biomass pool in CBM. As they are typically in contact with the upper forest floor, are assumed to be consumed at the same rate as coarse woody debris.

2.10 Calculation of Annual Direct C Emissions from Fire

To compute an estimate of the total direct C emissions from forest fires in Canada in 2023, the classified burn severity product from the National Burned Area Composite annual production was utilized (see Hall et al 2020 for an algorithm description). In NBAC, an internal tracking value "NFIREID" is utilized, which is the final satellite-derived burned area polygon (allowing for multi-part polygons) is split across any RU unit boundaries (if any). Since carbon pool sizes vary across RU boundaries, this allows for a single NFIREID to be present across multiple RUs.

A total of 2199 fires as small as 0.09 ha (one 30x30 landsat pixel) were mapped by NBAC for burn severity for a total of 14.60 Mha, but only fires over 100 ha were utilized as a lower limit of where meaningful per-fire estimates of the fraction of

low, moderate, and high severity burned area was available. Including only fires 100 ha and larger reduced the total number of fires to 966 but the total area remained largely the same at 14.58 Mha. A total of 189,704 ha of post-fire salvage logging was also mapped in 2023 and is assigned to the moderate severity class after consultation with provincial land managers. The direct C emissions from fire shown here are not altered by the act of post-fire salvage logging. Additionally, the NBAC mapping process accounts for unburned islands (and areas with a mapped fire severity no different than unburned) which count towards the total fire area but do not have a disturbance matrix and direct C estimate applied.

A unique DM was then calculated for each fire using the median area-weighted Drought Code per fire. All thermal detection hotspots from VIIRS that intersect a fire were extracted from the historical hotspot archive that supports the Canadian smoke emissions model CFFEPS-FireWork (Chen et al., 2019). The median DC value across all intersecting hotspots was used to derive a single DM per fire, no matter the duration of burning.

To compute total direct fire emissions per fire, a single estimate of the carbon pool size based on the Reporting Unit of the centroid of the NFIREID polygon was applied. Since polygons are split across RU boundaries, the spatial weighting of the pool size per fire is performed automatically. While spatially explicit biomass maps are available for some aboveground components (Guindon et al., 2024) and some organic soil components (Hanes et al., 2022), the majority of the required pool sizes in CBM for the computation of the fire DMs are available only at the spatially referenced RU scale.

3 Results and Discussion

Table 8. High severity Disturbance Matrix in BP

	Softwood Merchantable	Softwood Stem Snag	Medium DOM	Softwood Foliage	Aboveground Very Fast DOM	CO2	CH4	CO	PM25
Softwood Merchantable	0	1							
Softwood Stem Snag		0	0.45000			0.4774000	0.0027500	0.0385000	0.0104500
Medium DOM			0.57624			0.2979033	0.0055089	0.0682254	0.0169504
Softwood Foliage				0	0.00	0.8680000	0.0050000	0.0700000	0.0190000
Aboveground Very Fast DOM					0.02	0.8506400	0.0049000	0.0686000	0.0186200
CO2									
CH4									
CO									
PM25									

3.1 Direct fire carbon emissions as a function of fire severity and drought

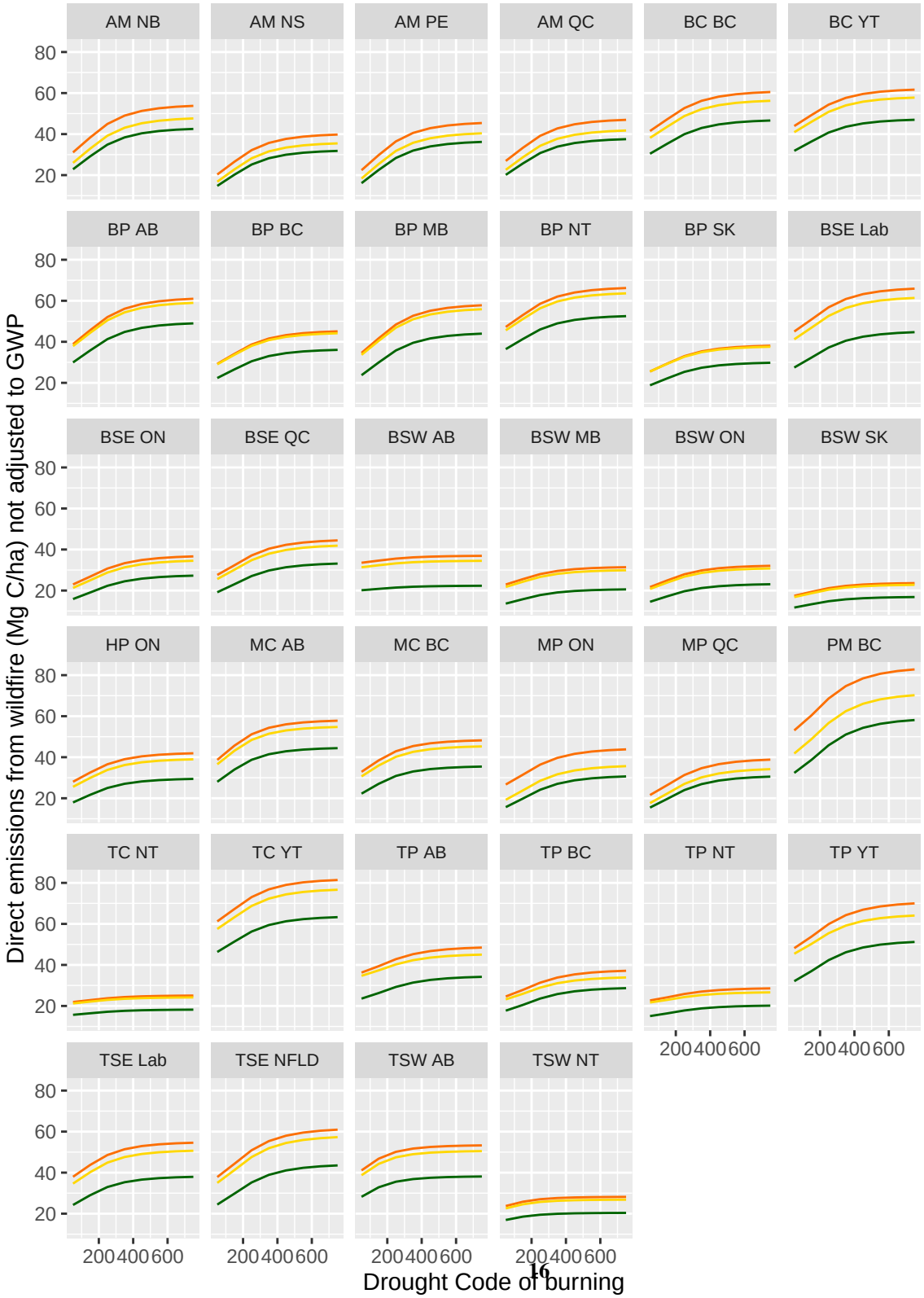

Direct emissions by severity class: orange = high, yellow = moderate, green = low severity. Labelled acron are Reporting Units (see Figure 1) as Ecozone then Province, so BC is both Boreal Cordillera and British Columba. Labrador is distinct from the island of Newfoundland for Reporting Units

Table 9. Comparison of the Modified Combustion Efficiency (MCE) of airborne gas measurements of Canadian wildfires against modelled MCE

Study	Date	Subset	Ecozone	Drought Code	Obs MCE	Modelled MCE
Hornbrook et al 2011	2008-07-01	Afternoon (0.2Low 0.4Mod 0.4High)	Boreal Shield West	250	0.92	0.912
Hornbrook et al 2011	2008-07-01	Late Evening (100% low severity)	Boreal Shield West	250	0.82	0.901
Hornbrook et al 2011	2008-07-04	After rain smouldering only low severity	Boreal Shield West	275	0.83	0.901

3.2 Comparison against observed direct fire emissions

3.2.1 Forest fire observations of CO and CO2 emissions ratios

Mean observed Modified Combustion Efficiency was observed by Hornbrook et al. (2011) for distinct periods during the ARCTAS campaign over northern Saskatchewan in 2008. MCE observed by aircraft during the peak burn period when the majority of fuel consumption and area burned occurs (0.92) largely corresponded with modelled values (0.91), suggesting the model provides a fair representation of the balance of flaming and smouldering during large active wildfires. Subsequent smoke plume observations during periods of greatly reduced spread and intensity (late evening and after rain) showed a substantially reduced MCE of 0.82-0.83 that indicates a near lack of flaming combustion. Even when represented as 100% low severity fire in the model, the modelled MCE only declines to 0.903. Since the fire DM model is based on area burned, fire activity such as smouldering but with minimal actual area burned increased is going to show an MCE far lower than areas of low severity fire spread, which are typically still a low sub-canopy flaming front that features a mix of smouldering duff and woody debris alongside flaming consumption of litter (McRae et al., 1994, 2017).

3.3 2023 Canadian wildfire season total direct emissions

!!! results table to be completed for the 2023 emissions !!!

A total of 501 Mt C was estimated to be released directly by fires in Canada in 2023. The total mass of PM2.5 emissions was estimated as 3.2284828×10^7 Mt of total mass, assuming a 50% carbon content.. The area-weighted mean Drought Code for all fires in Canada in 2023 was 444, representing severe but not uniformly exceptional drought conditions in Canada's northern forests. The area-weighted mean total C emissions per unit area was 34.36, though 90% of the emissions per unit area were between the 5th percentile of 14 t C/ha typical of the Taiga Plains ecozone under low drought conditions and the 95th percentile of 14 t C/ha typical of Pacific coastal forests.

Byrne et al 2024 used observed total atmospheric column excess CO and a range of MCE values to estimate total fire C emissions in Canada in 2023 of between 570-727 Mt C with a mean estimate of 647 Mt. The uncertainty in the estimate from Byrne et al 2024 lies primarily in the uncertain CO_2:CO ratio (more commonly computed as the normalized ratio MCE). Our bottom-up estimates that partition flaming vs smouldering shows a lower CO_2:CO estimate of 6.06. This lower CO_2:CO ratio (i.e. more smouldering) if applied to the data from Byrne et al 2024 would reduce their lower range of total C emissions

to 508.81 Mt C, which is comparable to the 501 Mt C computed from this bottom-up approach. Estimates of total carbon emissions based solely on the sum of observed Fire Radiative Power (FRP) from Copernicus-CAMS was approximately 490 Mt C (https://atmosphere.copernicus.eu/smoke-canadian-wildfires-reaches-europe)

3.3.1 Relationship to other fire carbon models

The forest floor emissions modelling scheme used here builds upon the CanFIRE model (de Groot et al., 2013) which incorporates a similar estimate of absolute forest floor emissions based on fuel type and various Fire Weather Index inputs (including but not limited to Drought Code). While the CanFIRE model is also capable of estimating tree mortality, the premise of CanFIRE lies in the use of the Canadian fire Behaviour Prediction (FBP) System to model fire intensity and a physiological-thermodynamic model of tree damage and mortality. CanFIRE is able to run entirely in scenario or forecast mode, i.e. no fire severity map is needed to run the model, unlike the focus here on a mechanism to estimate carbon fluxes and pools after fire severity is mapped. Ultimately, models like CanFIRE can be used for near-real time emissions estimates of direct and indirect fire carbon emissions (and also for prescribed fire planning and scenario testing), while this modelling framework is best used solely operational carbon accounting and reporting given its strong dependence severity maps. While fire severity can be estimated empirically based on geospatial inputs without observation using multispectral satellite data such as Landsat !!![Ellen's paper?]!!!, estimation using coupled fire behaviour and ecology models such as CanFIRE is a more direct approach. Under severe drought conditions and light winds, very large fires often create more wind and energy than is available in gradient winds as measured at nearby airports and fire weather observing stations !!!(cite Coen paper on fire-induced winds)!!! Thus, fire behaviour and fuel consumption models solely driven by wind inputs from distant meteorological stations can under-predict fire intensity and therefore likely fire severity. While fire-atmosphere models are available for research !![cite coen again] and some forecasting and planning purposes (Linn et al., 2020), modelling resources are typically not made available for the extensive and largely unsuppressed fires in northern Canada. Fire severity mapping after the fact is able to account for high fire severity (Whitman et al., 2018) even when fire spread occurs under light winds (Whitman et al., 2024).

While the fire DMs presented here are designed for use in the CFS-CBM carbon reporting framework, their simplicity and similarity to many other forest carbon schema allows them to be used elsewhere such as in other forest dynamics (Brecka et al., 2020) and earth system models (Melton et al., 2020) that require estimates of Canadian forest carbon emissions from wildfire. Stenzel et al. (2019) showed that severity-informed fire C estimates (with snags) in the US are only 30-40% as large as fixed or variable severity data using their LANDIS-type models. Large over-estimates of in-fire bole consumption in models were not observed to correspond to measurements in the field. In the model presented here, our estimates of snag consumption are based on simple but logical relationships with Crown Fraction Burned, but more comprehensive data collection and field observations would be required to extend the accuracy of the snag consumption scheme.

3.3.2 Indirect fire emissions

While fire emissions within the year of the fire are majority of the GHG flux, enhanced post-fire decomposition of dead biomass persists for many years after a fire. The increase in post-fire tree mortality between the year of the fire and the year following

the fire is as much as 30% in low and moderate-severity stands (Angers et al., 2011). This extended mortality is not captured in year-of fire severity mapping but is likely better assessed using fire severity data captured the year following fire, as is operation practice in Canada !!!![cite Ellen's upcoming paper]!!!. Similarly, the transition of fire-killed stems (snags) from upright to the forest floor woody debris takes between 5-8 years for 50% of stems to fall (Angers et al., 2011) with stemfall rate highest in low-severity fire. Field observations show that initial assessments of fire severity are the primary predictors of snag fall Angers et al. (2011) and decomposition (Boulanger et al., 2011) rates, meaning the mapped severity method used here provides a useful input for multi-year fire carbon modelling of the snag pool in CBM. For organic soil pools, fire has been shown to suppress decomposition rates in upland soil pools where drier post-fire conditions are present (Holden et al., 2015), while in permafrost upland (O'donnell et al., 2011) and peatland (Gibson et al., 2018, 2019) systems, fire has profound impacts on soil carbon pools by rapidly increasing thaw depths and subsequent decomposition rates. Currently in CBM, decomposition rates are calibrated against field decomposition litterbag experiments (Trofymow et al., 2002) and annual climate metrics that do not take into account how disturbances such as fire (and fire of varying severity) modify decomposition rates in the absence of a change in climate.

3.3.3 Model gaps

Currently, the model framework only accounts of regionally-averaged soil carbon stocks, meaning that Reporting Units with high peatland areas will show higher organic soil slow pool size (see Table ###), but peatlands themselves are not spatially represented in the model. Currently, fire disturbance in peatlands is performed by the CaMP model, which uses the same Drought Code fire weather metric to estimate peat layer consumption (Bona et al., 2020) and uses the overstory carbon schema of CBM to estimate overstory tree carbon pools and fluxes. Direct satellite monitoring of upland forest organic soil and peatland carbon loss via burn severity monitoring is possible but remains a challenge to implement with accuracy for monitoring purposes (Bourgeau-Chavez et al., 2020). Despite the large carbon stock, the mean C emissions per area in peatland due to fire (65 t C/ha) as modelled by Bona et al. (2024) are comparable to regional emissions from peat-rich ecozones such as the Boreal and Taiga Plains under moderate to severe drought conditions. Indeed, it is under these moderate to severe drought conditions under which peatlands burn more frequently (Turetsky et al., 2004; Thompson et al., 2019) and severely (Kuntzemann et al., 2023).

This algorithm is currently built off of regionally averaged biomass pools by Reporting Unit (Figure 1; Appendix ###). While Canadian wildfires shown an overall selection bias towards preferentially burning older conifer stands (Bernier et al., 2016), fuel selectivity against less flammable portions of the landscape decreases strongly under severe drought conditions (Parks et al., 2018) such as those experienced in Canada in 2023 (Jain et al., 2024) where we performed the algorithm validation against independent fire emissions observations. Algorithm evaluation against individual fires or years of less profound drought would be more likely to highlight the limitation of the regionally-averaged carbon pool (i.e. fuel load) values used here. Ultimately, the mapped severity used here is best paired with mapped carbon pools at a similar scale, such as the 1-ha forest carbon modelling for analysis and scenario testing used by Smyth et al. (2024).

Species-specific traits in trees with overlapping ranges, such as resprouting is aspen (Brown and DeByle, 1987) but not other broadleaves such as oak or maple, are not explicitly handled in this model. Instead, the relative abundance of trees with contrasting traits that influence ecological outcomes such as fire survival are lumped at the ecozone scale from the aggregation of the plot data. While ecozone-level contrasts in key considerations such as overstory mortality do strongly vary by ecozone !!!![Table ###], the same DM (e.g. hardwood root mortality) is applied in adjacent stands at the same severity class despite the potential for strongly contrasting traits that are readily tied back to mapping at the stand level by leading species. Alternately, models such as CanFIRE can account for species-level contrasts in fire ecology traits, but compiling the relevant ecophysiological properties and traits for all tree species in Canada remains incomplete at the current time.

4 Conclusions

Carbon emissions from wildfires in Canada represent a substantial pulse input of greenhouse gases to the atmosphere: the 2023 fire emissions in Canada were an input of approximately 501 Mt C. A modelling framework to extend the current fire and greenhouse gas reporting in Canada is presented. In contrast to the existing modelling system that utilizes a fixed fire severity (i.e. tree mortality) assumption, a field-calibrated satellite fire severity mapping process that follows mature and well-established scientific methods is used. Above-ground carbon pool changes (from live to dead and in situ as well as to the gas phase) rely on a robust field observation dataset that relates back to satellite metrics. Evaluation of the modelling presented above against fully independent airborne observations of CO:CO_2 emissions ratios for boreal wildfires indicates the modelling of proportion of flaming vs smouldering emissions are well-replicated by the model. With confidence in this modelled CO:CO_2 ratio, the total fire CO emissions for the 2023 wildfire season in Canada (with a record 15 Mha burned) is broadly consistent with fire season estimates using satellite total column CO anomalies.

While this prototype carbon flux framework utilizes regionally-averaged carbon stock estimates, future systems deployment within Canada's carbon accounting system is likely to incorporate precisely mapped (1 ha) carbon pools alongside the finely mapped fire severity products (30 m) used here. As both the spatial estimates of carbon stocks across Canada's forested ecosystems improves alongside additional field observations, it is anticipated that this modelling framework will increase in both accuracy and precision over time.

5 Appendix A: Mean pool size by Reporting Unit

6 Appendix B: non-linear least squares modelling of soil organic layer consumption

For national annual estimates of forest organic soil layer consumption during wildfire, implementations that only utilize Canadian experimental fire data from the Fire Behaviour Prediction System will be limited to a maximum consumption value of 5 kg (biomass) m^{-2} of total surface fuel (woody debris, litter, and duff) of 5 kg m^{-2}, or 25 Mg C ha^{-1}, given the observation dataset and fitted model parameters. For the common "C-2" boreal spruce fuel type for instance, Surface Fuel Consumption, SFC (biomass units in kg m^{-2} not kg C) is modelled as:

$$SFC = 5.0\left(1 - e^{-0.0115BUI}\right)^{1.0} \quad (8)$$

This model form has the distinct advantage of SFC being 0.0 at a BUI of zero. The model parameters vary by fuel type (i.e. deciduous broadleaf fuels are limited to 1.5 kg m^{-2} of maximum SFC) but are fixed within a fuel type.

More recent observations and modelling from de Groot et al. (2009) extended the FBP data with an additional 128 observations from 7 additional wildfires, and the ABoVE project compiled over 1,000 field observations of depth of burn and C stocks before and after wildfire in Canada and Alaska, over 600 of which are in North American Level II ecoregions also occurring in Canada (Walker et al., 2020). de Groot et al. (2009) provides a concise and informative improvement on the FBP fuel consumption equations, where both a Fire Weather Index System component (in this case, Drought Code) is used similarly to Buildup Index in the FBP, but importantly, the site-level organic soil layer fuel load is also accounted for, which allows for the greater absolute combustion in deeper organic soils that is moderated by the natural logarithm transformation:

$$log_e(FFFC) = -4.252 + 0.710log_e(DC) + 0.671log_e(FFFL) \quad (9)$$

where FFFC is Forest Floor Fuel Consumption (SFC minus surface woody debris) in kg (biomass) m^{-2} and FFFL is Forest Floor Fuel Load in kg m^{-2}. The forest floor as defined here is inclusive of the litter and duff layers, live mosses and lichens. This model presented above fits well within the dataset and extends the observed maximum FFFC to nearly 10 kg m^{-2}. The ABoVE synthesis of FFFL and FFFC (Walker et al 2020 ORNL) expands upon a slightly smaller dataset used in a modelling summary also by Walker et al (2020 NCC), where structural equation modelling was used to explore drivers of FFFC but no concise and readily reproducible modelling is produced. The results of the SEM from Walker et al (2020 NCC) emphasized a greater role of FFFL over DC, though coarse reanalysis that lacked local fire agency weather stations was used. An analysis of just 2014 fires in the Northwest Territories by (walker2018) showed that while the mean depth of burn across all black spruce stands was 6-10 cm, the driest (xeric) black spruce stands with the smallest FFFL showed upwards of 75% soil organic consumption, while deeper organic soils in subhygric black spruce stands showed less than 25% consumption.

To provide the largest possible dataset for FFFC and FFFL, the ABoVE synthesis was combined with wildfire data from de Groot et al 2009 not otherwise found in the ABoVE synthesis. The ABoVE synthesis sites in the Alaska Boreal Interior ecoregion, which have equivalent Canadian ecozone were excluded, but Alaska Boreal Cordillera sites near the Yukon border were utilized. Experimental fire data from the FBP data was not used, as deeper combustion measurements resulting from hours and days of smouldering combustion captured in wildfire data are not available in experimental fires where extensive smouldering is not measured due to suppression. In order to best represent on-the-ground Fire Weather Index values, the Drought Code and other FWI values from Walker et al 2020 reanalysis were substituted with interpolated weather station (both Environment and Climate Change Canada as well fire agency stations). This data also has the benefit of being properly overwintered for Drought Code (Hanes DC overwinter) and capturing small rain events not captured in reanalysis that meaningfully impact the Duff Moisture Code in particular.

For the purposes of improving national estimates of the fractional soil organic layer loss during wildfire, this framework emphasizes the proportional C stock loss (as with all CBM disturbance matrices) rather than the absolute value of combustion. In contrast to the modelling of absolute combustion value, any analysis of proportions is best conducted as logit- transformed data, where the logit transformation is:

$$logit(p) = log\frac{p}{1-p} \tag{10}$$

which effectively transforms a data of proportions of [0,1] to a Gaussian distribution with a range of approximately -5 to +5 (in this dataset), and a mode approximately at zero. Within the logit-transformed data, exploratory analysis of ecozones as a factor alongside other non-linear splines of FWI values and FFFL was conducted:

```
##
## Family: gaussian
## Link function: identity
##
## Formula:
## prop_sol_combusted_logit ~ s(drought_code, k = 4, bs = "tp") +
##     ecozone + s(AGSlow.Mg.C.ha, k = 4, bs = "tp")
##
## Parametric coefficients:
##             Estimate Std. Error t value Pr(>|t|)
## (Intercept)  0.11939    0.09318   1.281   0.2005
## ecozoneBP   -0.29433    0.15506  -1.898   0.0581 .
## ecozoneBSW  -0.19928    0.15988  -1.246   0.2131
## ecozoneTP   -0.23049    0.11476  -2.008   0.0450 *
## ecozoneTSW  -0.29887    0.12157  -2.458   0.0142 *
## ---
## Signif. codes:  0 '***' 0.001 '**' 0.01 '*' 0.05 '.' 0.1 ' ' 1
##
## Approximate significance of smooth terms:
##                     edf Ref.df       F p-value
## s(drought_code)   1.352  1.618   2.862  0.0631 .
## s(AGSlow.Mg.C.ha) 2.950  2.998 232.720  <2e-16 ***
## ---
## Signif. codes:  0 '***' 0.001 '**' 0.01 '*' 0.05 '.' 0.1 ' ' 1
##
```

```
## R-sq.(adj) =  0.628   Deviance explained = 63.3%
## -REML = 869.04  Scale est. = 0.81207   n = 651
```

(could also show boxplots?) which shows that the Boreal Cordillera ecozone has a meaningfully higher proportional soil organic layer consumption rate compared to BP, BSW, TP, and TSW, all of which are not significantly different in consumption rates once DC and FFFC (shown as AGSlow.Mg.C.ha) are accounted for. Boreal Cordillera data were set aside for a distinct model.

Similar to de Groot et al. (2009), Drought Code was a better predictor of consumption rates than Buildup Index as used in the FBP. In the logit transformed space, saturation-type non-linear curve using the relevant FWI component was fitted in a non-linear least squares model, but an additive term of the natural-logarithm transformed FFFC (given as AGSlow pool in Mg C/ha) was used as well. In the end, a superior model was found using the proportional depth of burn, rather than the proportional loss of the mass of the soil organic layer. The non-linear least squares model fit was conducted using the Levenberg-Marquardt nonlinear least-squares algorithm found in MINPACK (Elzhov et al 2023) R package, which supported bounded parameter constraints.

In the abstract, the model follows the form:

$$logit\left(\frac{depthofburn}{pre-fireorganicdepth}\right) = [c(1-e^{(aDC)})] + (blog_e(AGSlow)) \tag{11}$$

with fitted parameters as:

$$logit\left(\frac{depthofburn}{pre-fireorganicdepth}\right) = [3.83(1-e^{(-0.005DC)})] + (-0.718log_e(AGSlow)) \tag{12}$$

Note the "b" coefficient on the parameter associated with the FFFL (AGSlow) of -0.718, which results in larger organic layer fuel loads leading to smaller proportional consumption values, which follows the patterns shown by Walker 2018 for NWT fires of 2014.

The a parameter term that forms the exponent of e alongside Drought Code is related to the DC value at which half of the maximum possible asymptotal consumption value is observed (for a given FFFL value). The NLS fitting was given a minimum value of -0.06 such that half of the asymptotal maximum consumption rate was modelled as occurring at or around a DC value of 300. The other parameters were fit to the best possible value with no constraint.

Importantly, since fire behaviour, emissions modelling, and carbon accounting all operate with the calculation of mass loss and depth of burn, a correction factor was applied that corrects for the trends in bulk density with depth for C-2 fuels as given by de Groot et al. (2009), so that a model of proportional depth of burn is then converted into a proportional mass loss term:

$$\left(\frac{FFFC}{FFFL}\right) = 1.017\left(\frac{depthofburn}{pre-fireorganicdepth}\right)^{0.250} \tag{13}$$

which for example means that the median proportional depth of burn in the AboVE/de Groot training data of 0.40 corresponds to 0.32 of the proportional mass loss (since shallow organic soil is less dense), or a correction factor of 0.80. For non-spruce-dominated fuels, this correction is much smaller but still meaningful:

$$\left(\frac{FFFC}{FFFL}\right) = 0.13\left(\frac{depthofburn}{pre-fireorganicdepth}\right) + 0.87 \tag{14}$$

(show perhaps what a few different a values look like?) (also compute the DC value of about half the maximum FBP SFC values too, just for kicks)

For example, using a moderately thick ~12 cm thick organic soil layer, the proportion of consumption as a function of Drought Code using the model above

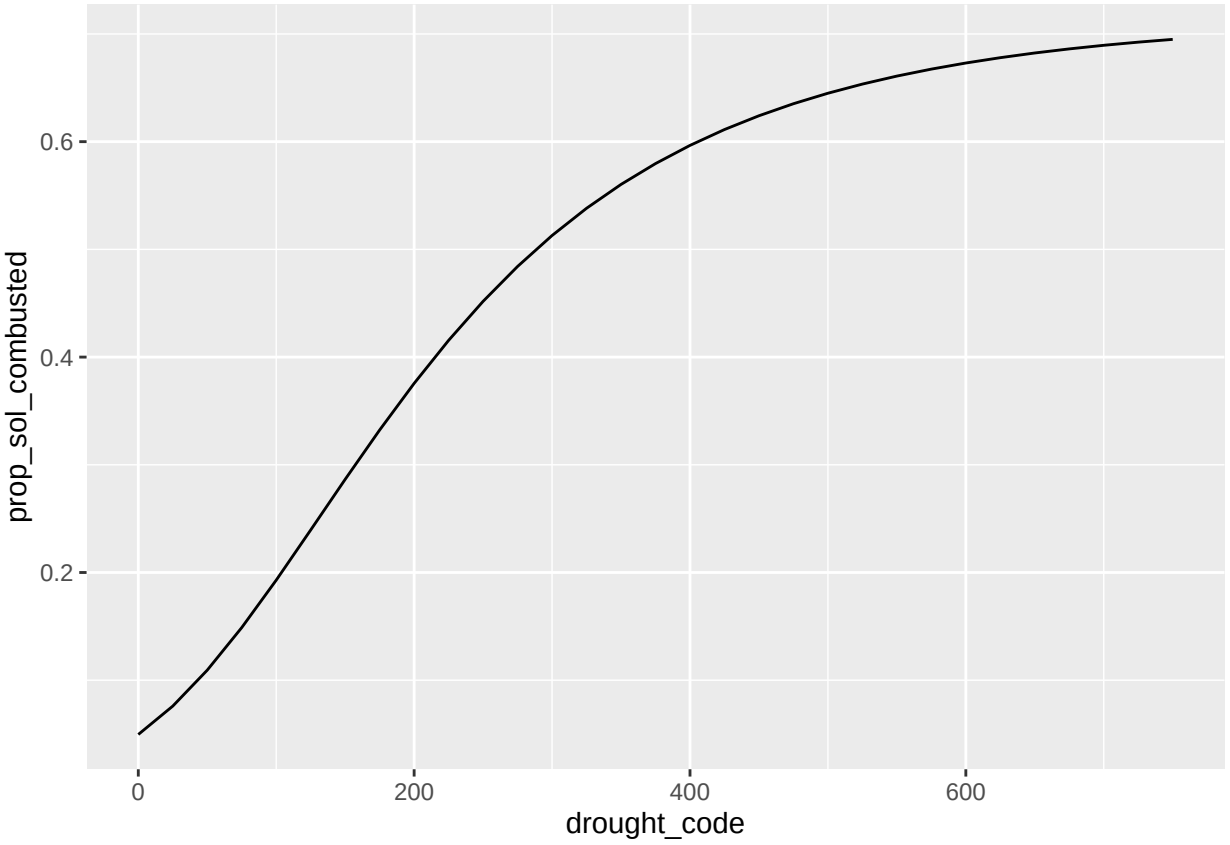

With the parameter constrained NLS fitting, the proportional consumption model for the forest floor has a leave-one-out (conducted at the fire-level, not plot) cross validated r2 of ###, and a Mean Percent Error of ###%

```
## Scale for y is already present.
## Adding another scale for y, which will replace the existing scale.
## Scale for y is already present.
```

```
## Adding another scale for y, which will replace the existing scale.
## Scale for x is already present.
## Adding another scale for x, which will replace the existing scale.
```

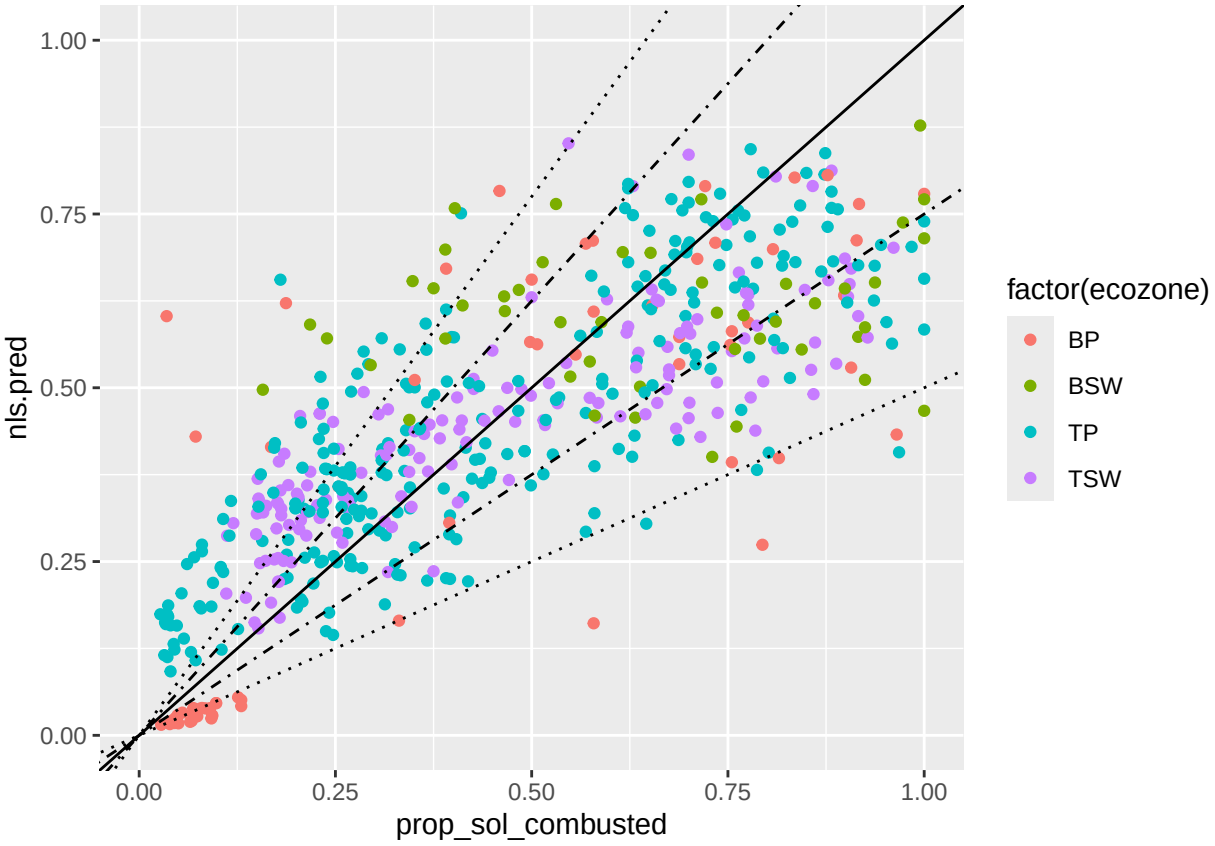

475

Across the entire parameter space of Drought Code and AGSlow pool size, the following isolines of proportional consumption in the model can be plotted:

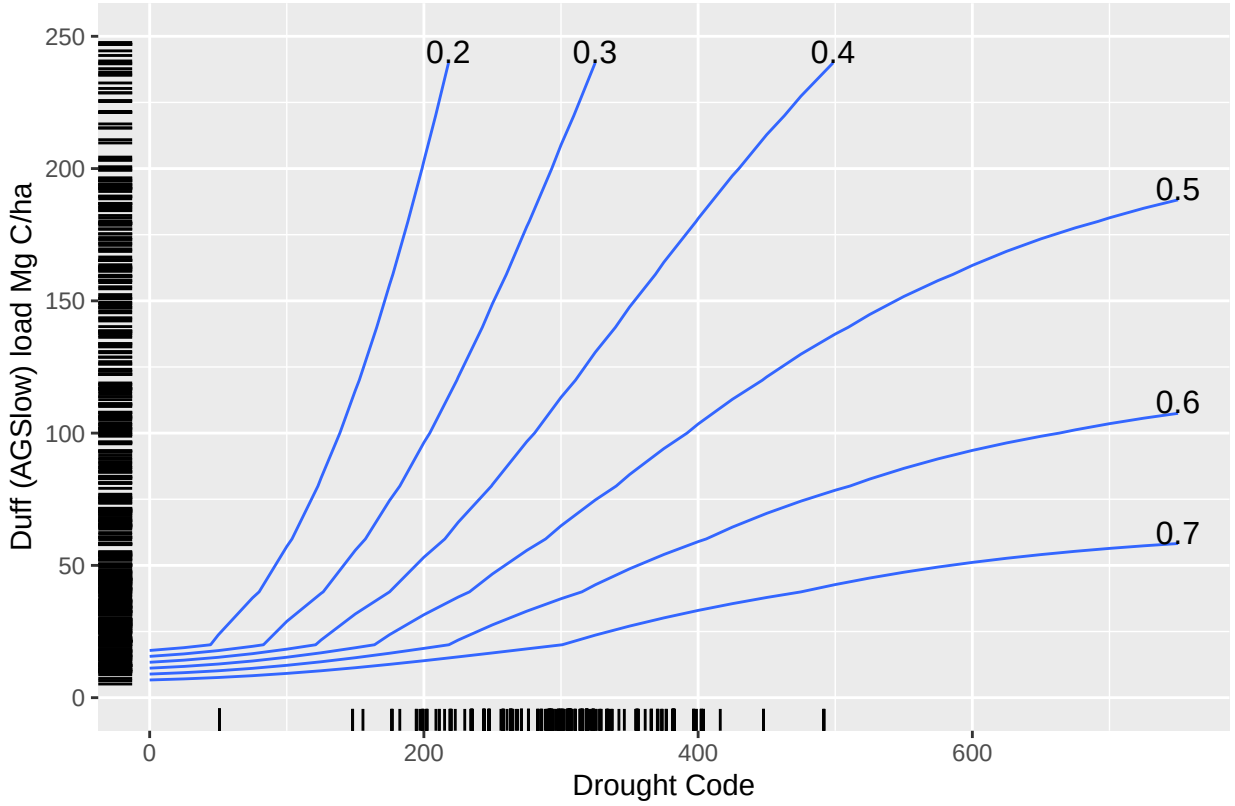

Isoline contours of equal organic soil layer consumption fraction as a function of Drought Code and the orgar

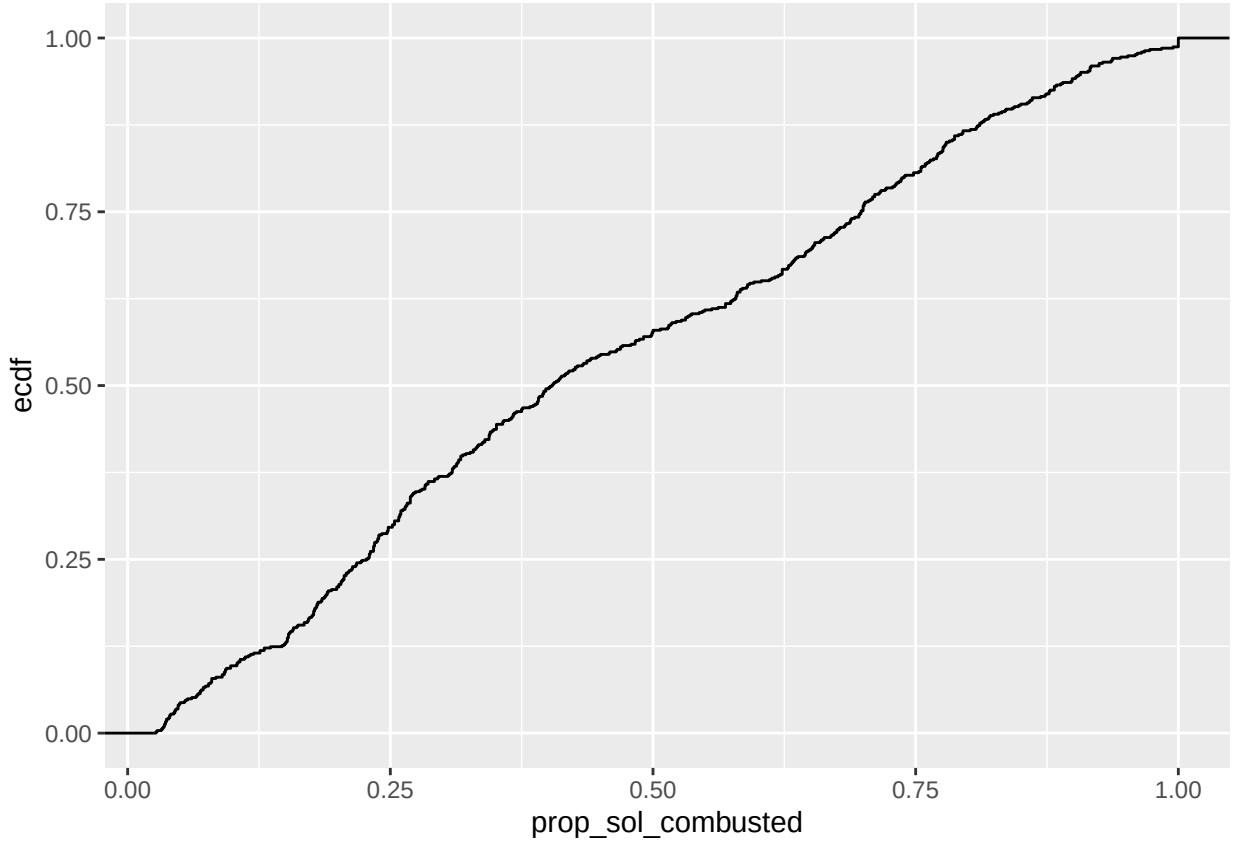

6.0.1 Boreal Cordillera modelling

For the Boreal Cordillera, a simple linear model on the logit-transformed data was found to be the best performing model for estimating soil organic consumption proportion:

$$logit\left(\frac{FFFC}{FFFL}\right) = (0.00257 * DC) + (-0.54 * log_e(AGSlow)) + 2.17 \quad (15)$$

Despite the presence of a fixed intercept term, the strong inverse dependence on the natural logarithm of the AGSlow pool size (FFFL) results in zero proportional consumption when Drought Code is equal to zero.

7 Appendix C: annual variability in observed Drought Code during wildfire spread, and impact on ecozone-level average forest floor emissions

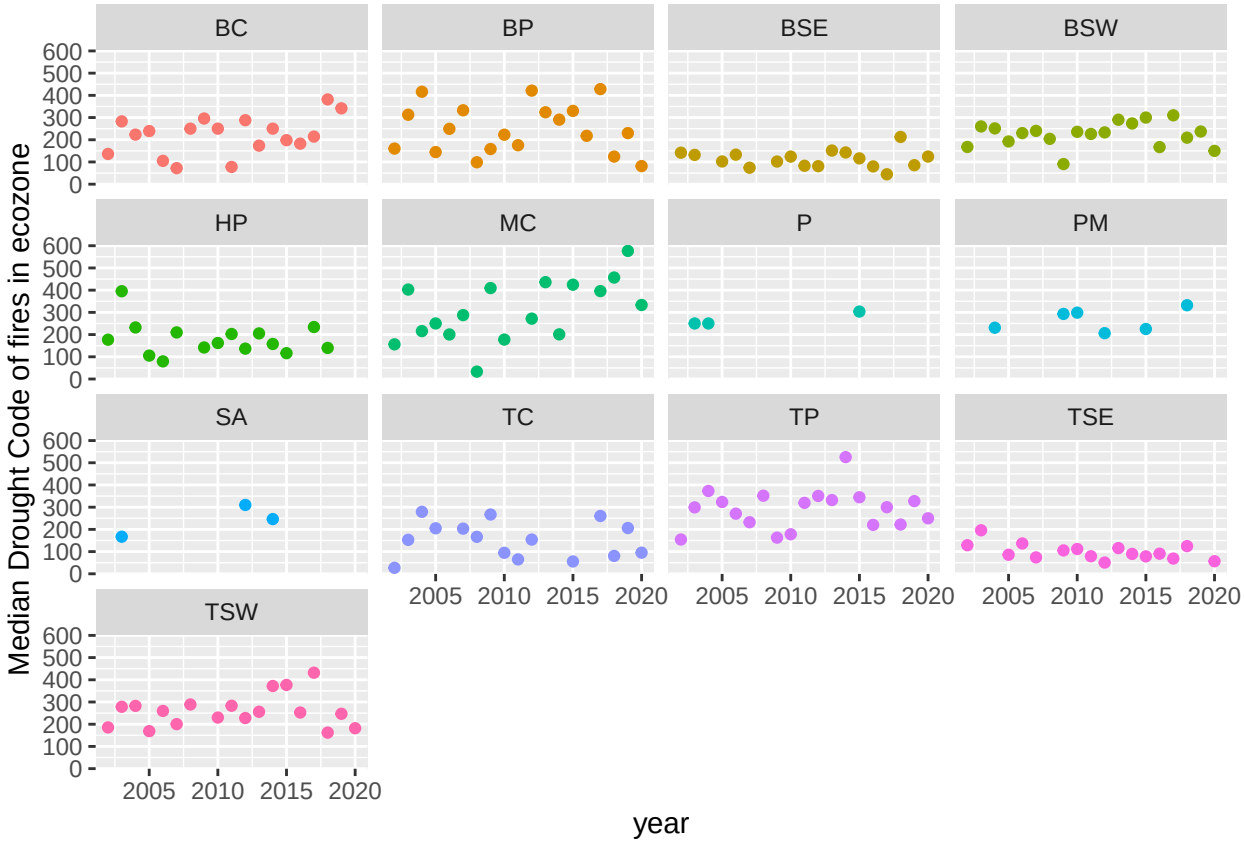

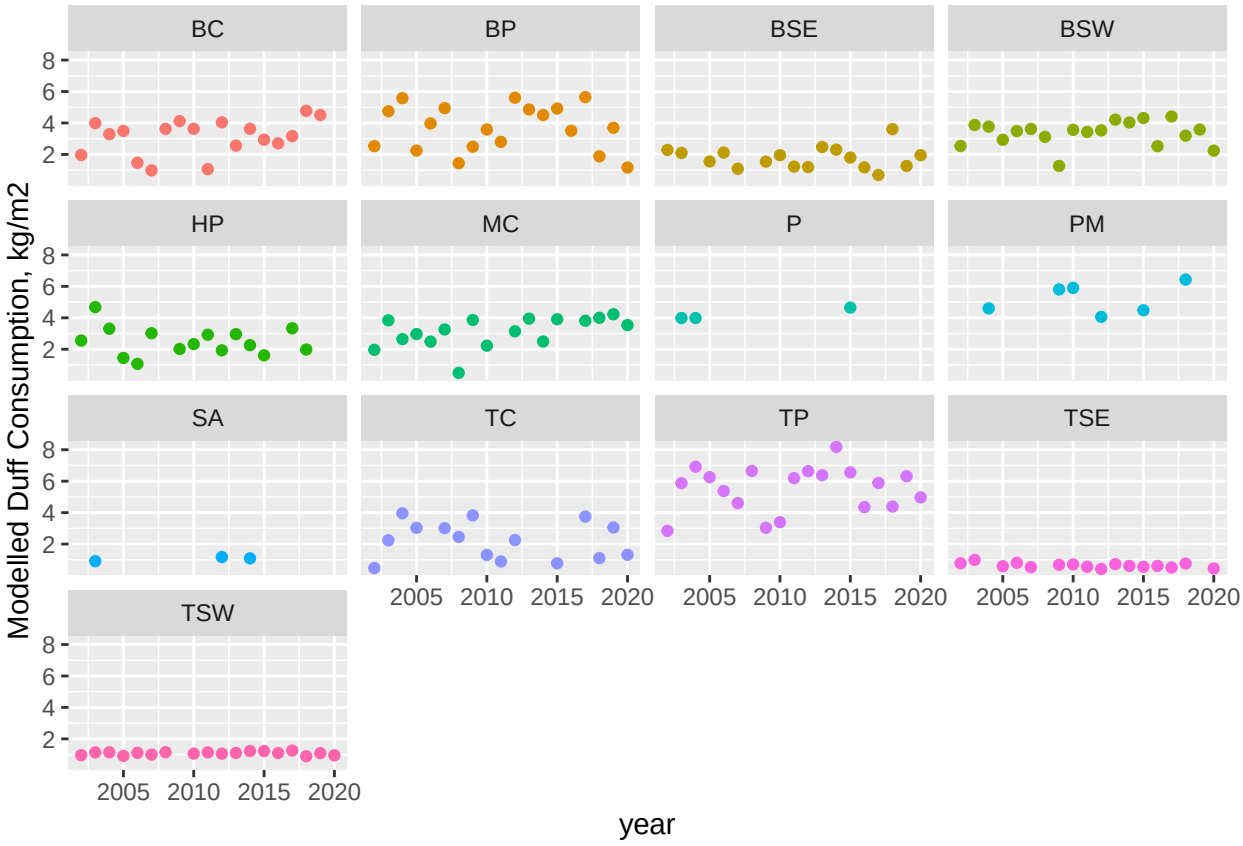

8 Appendix D: Representative photos

Photos of: (1) partial litter consumption; (2) partial vs full duff consumption; (3) mortality but not consumption of understory trees with live overstory; (4) mortality but not consumption of overstory trees; (5) mixedwood severity example showing consumption of broadleaf foliage; (6) woody debris consumption; (7) snag preferential consumption relative to little to no bole consumption in live trees

Give lat/long, year, ecozone, severity class, and leading spp for each photo, maybe other relevant metrics? From some of the experimental fires mostly??

9 Appendix E: List of Resprouting Hardwoods of Canada

Alnus spp. Arbutus men. Betula all. Betula pap. Betula pop. Fraxinus ame. Fraxinus nig. Fraxinus pen. Populus bal. Populus gra. Populus tre. Populus tri. Quercus spp. Salix spp.

. This article was produced from an RMarkdown document with underlying data, available at https://github.com/nrcan-cfs-fire/FireDMs

. The authors declare no competing interests.

. The algorithm and results presented only apply to boreal and temperate forest ecosystems where sufficient ground plots of fire severity are available. As a data-driven model, this framework is not suitable for other ecosystems nor agricultural or forestry biomass burning practices.

References

Angers, V. A., Gauthier, S., Drapeau, P., Jayen, K., Bergeron, Y., Angers, V. A., Gauthier, S., Drapeau, P., Jayen, K., and Bergeron, Y.: Tree mortality and snag dynamics in North American boreal tree species after a wildfire: a long-term study, International Journal of Wildland Fire, 20, 751–763, https://doi.org/10.1071/WF10010, publisher: CSIRO PUBLISHING, 2011.

Barber, Q. E., Jain, P., Whitman, E., Thompson, D. K., Guindon, L., Parks, S. A., Wang, X., Hethcoat, M. G., and Parisien, M.-A.: The Canadian Fire Spread Dataset, Scientific Data, 11, 764, https://doi.org/10.1038/s41597-024-03436-4, 2024.

Benscoter, B. W., Thompson, D. K., Waddington, J. M., Flannigan, M. D., Wotton, B. M., Groot, W. J. d., and Turetsky, M. R.: Interactive effects of vegetation, soil moisture and bulk density on depth of burning of thick organic soils, International Journal of Wildland Fire, 20, 418–429, https://doi.org/10.1071/WF08183, 2011.

Bernier, P. Y., Gauthier, S., Jean, P.-O., Manka, F., Boulanger, Y., Beaudoin, A., and Guindon, L.: Mapping Local Effects of Forest Properties on Fire Risk across Canada, Forests, 7, 157, https://doi.org/10.3390/f7080157, 2016.

Bona, K. A., Shaw, C., Thompson, D. K., Hararuk, O., Webster, K., Zhang, G., Voicu, M., and Kurz, W. A.: The Canadian model for peatlands (CaMP): A peatland carbon model for national greenhouse gas reporting, Ecological Modelling, 431, 109 164, https://doi.org/10.1016/j.ecolmodel.2020.109164, 2020.

Bona, K. A., Webster, K. L., Thompson, D. K., Hararuk, O., Zhang, G., and Kurz, W. A.: Using the Canadian Model for Peatlands (CaMP) to examine greenhouse gas emissions and carbon sink strength in Canada's boreal and temperate peatlands, Ecological Modelling, 490, 110 633, https://doi.org/10.1016/j.ecolmodel.2024.110633, 2024.

Boulanger, Y., Sirois, L., and Hébert, C.: Fire severity as a determinant factor of the decomposition rate of fire-killed black spruce in the northern boreal forest, Canadian Journal of Forest Research, 41, 370–379, https://doi.org/10.1139/X10-218, publisher: NRC Research Press, 2011.

Bourgeau-Chavez, L. L., Grelik, S. L., Billmire, M., Jenkins, L. K., Kasischke, E. S., and Turetsky, M. R.: Mapping Boreal Peatland Fire Severity and Assessing their Potential Vulnerability to Early Season Wildland Fire, Frontiers in Forests and Global Change, 3, https://doi.org/10.3389/ffgc.2020.00020, 2020.

Brecka, A. F. J., Boulanger, Y., Searle, E. B., Taylor, A. R., Price, D. T., Zhu, Y., Shahi, C., and Chen, H. Y. H.: Sustainability of Canada's forestry sector may be compromised by impending climate change, Forest Ecology and Management, 474, 118 352, https://doi.org/10.1016/j.foreco.2020.118352, 2020.

Brown, J. K. and DeByle, N. V.: Fire damage, mortality, and suckering in aspen, Canadian Journal of Forest Research, 17, 1100–1109, https://doi.org/10.1139/x87-168, publisher: NRC Research Press, 1987.

Chen, J., Anderson, K., Pavlovic, R., Moran, M. D., Englefield, P., Thompson, D. K., Munoz-Alpizar, R., and Landry, H.: The FireWork v2.0 air quality forecast system with biomass burning emissions from the Canadian Forest Fire Emissions Prediction System v2.03, Geoscientific Model Development, 12, 3283–3310, https://doi.org/https://doi.org/10.5194/gmd-12-3283-2019, 2019.

de Groot, W., Pritchard, J., and Lynham, T.: Forest floor fuel consumption and carbon emissions in Canadian boreal forest fires, Canadian Journal of Forest Research, 39, 367–382, https://doi.org/10.1139/X08-192, 2009.

de Groot, W., Hanes, C. C., and Wang, Y.: Crown fuel consumption in Canadian boreal forest fires, International Journal of Wildland Fire, https://doi.org/10.1071/WF21049, 2022.

de Groot, W. J., Flannigan, M. D., and Cantin, A. S.: Climate change impacts on future boreal fire regimes, Forest Ecology and Management, 294, 35–44, https://doi.org/10.1016/j.foreco.2012.09.027, 2013.

Gibson, C. M., Chasmer, L. E., Thompson, D. K., Quinton, W. L., Flannigan, M. D., and Olefeldt, D.: Wildfire as a major driver of recent permafrost thaw in boreal peatlands, Nature Communications, 9, 1–9, https://doi.org/10.1038/s41467-018-05457-1, 2018.

Gibson, C. M., Estop-Aragonés, C., Flannigan, M., Thompson, D. K., and Olefeldt, D.: Increased deep soil respiration detected despite reduced overall respiration in permafrost peat plateaus following wildfire, Environmental Research Letters, 14, 125 001, https://doi.org/10.1088/1748-9326/ab4f8d, 2019.

Group, F. C. F. D. R.: Development and structure of the Canadian Forest Fire Behavior Prediction System, vol. ST-X-3, Forestry Canada, https://cfs.nrcan.gc.ca/publications?id=10068, 1992.

Guindon, L., Manka, F., Correia, D. L., Villemaire, P., Smiley, B., Bernier, P., Gauthier, S., Beaudoin, A., Boucher, J., and Boulanger, Y.: A new approach for Spatializing the CAnadian National Forest Inventory (SCANFI) using Landsat dense time series, Canadian Journal of Forest Research, https://doi.org/10.1139/cjfr-2023-0118, 2024.

Hall, R. J., Freeburn, J. T., Groot, W. J. d., Pritchard, J. M., Lynham, T. J., Landry, R., Hall, R. J., Freeburn, J. T., Groot, W. J. d., Pritchard, J. M., and et al.: Remote sensing of burn severity: experience from western Canada boreal fires, International Journal of Wildland Fire, 17, 476–489, https://doi.org/10.1071/WF08013, 2008.

Hall, R. J., Skakun, R. S., Metsaranta, J. M., Landry, R., Fraser, R. H., Raymond, D., Gartrell, M., Decker, V., and Little, J.: Generating annual estimates of forest fire disturbance in Canada: the National Burned Area Composite, International Journal of Wildland Fire, https://doi.org/10.1071/WF19201, 2020.

Hanes, C. C., Wang, X., Jain, P., Parisien, M.-A., Little, J. M., and Flannigan, M. D.: Fire-regime changes in Canada over the last half century, Canadian Journal of Forest Research, 49, 256–269, https://doi.org/10.1139/cjfr-2018-0293, 2019.

Hanes, C. C., Wang, X., Groot, W. J. d., Hanes, C. C., Wang, X., and Groot, W. J. d.: Dead and down woody debris fuel loads in Canadian forests, International Journal of Wildland Fire, 30, 871–885, https://doi.org/10.1071/WF21023, publisher: CSIRO PUBLISHING, 2021.

Hanes, C. C., Wotton, M., Woolford, D. G., Martell, D. L., and Flannigan, M.: Mapping organic layer thickness and fuel load of the boreal forest in Alberta, Canada, Geoderma, 417, 115 827, https://doi.org/10.1016/j.geoderma.2022.115827, 2022.

Hayden, K., Li, S.-M., Liggio, J., Wheeler, M., Wentzell, J., Leithead, A., Brickell, P., Mittermeier, R., Oldham, Z., Mihele, C., Staebler, R., Moussa, S., Darlington, A., Steffen, A., Wolde, M., Thompson, D., Chen, J., Griffin, D., Eckert, E., Ditto, J., He, M., and Gentner, D.: Reconciling the total carbon budget for boreal forest wildfire emissions using airborne observations, Atmospheric Chemistry and Physics Discussions, pp. 1–62, https://doi.org/10.5194/acp-2022-245, publisher: Copernicus GmbH, 2022.

Hessburg, P. F., Miller, C. L., Parks, S. A., Povak, N. A., Taylor, A. H., Higuera, P. E., Prichard, S. J., North, M. P., Collins, B. M., Hurteau, M. D., Larson, A. J., Allen, C. D., Stephens, S. L., Rivera-Huerta, H., Stevens-Rumann, C. S., Daniels, L. D., Gedalof, Z., Gray, R. W., Kane, V. R., Churchill, D. J., Hagmann, R. K., Spies, T. A., Cansler, C. A., Belote, R. T., Veblen, T. T., Battaglia, M. A., Hoffman, C., Skinner, C. N., Safford, H. D., and Salter, R. B.: Climate, Environment, and Disturbance History Govern Resilience of Western North American Forests, Frontiers in Ecology and Evolution, 7, https://doi.org/10.3389/fevo.2019.00239, 2019.

Holden, S. R., Berhe, A. A., and Treseder, K. K.: Decreases in soil moisture and organic matter quality suppress microbial decomposition following a boreal forest fire, Soil Biology and Biochemistry, 87, 1–9, https://doi.org/10.1016/j.soilbio.2015.04.005, 2015.

Hood, S. and Lutes, D.: Predicting Post-Fire Tree Mortality for 12 Western US Conifers Using the First Order Fire Effects Model (FOFEM), Fire Ecology, 13, 66–84, https://doi.org/10.4996/fireecology.130290243, 2017.

Hornbrook, R. S., Blake, D. R., Diskin, G. S., Fried, A., Fuelberg, H. E., Meinardi, S., Mikoviny, T., Richter, D., Sachse, G. W., Vay, S. A., and et al.: Observations of nonmethane organic compounds during ARCTAS Part 1: Biomass burning emissions and plume enhancements, Atmospheric Chemistry and Physics, 11, 11 103–11 130, https://doi.org/10.5194/acp-11-11103-2011, 2011.

Jain, P., Barber, Q. E., Taylor, S. W., Whitman, E., Castellanos Acuna, D., Boulanger, Y., Chavardès, R. D., Chen, J., Englefield, P., Flannigan, M., and et al.: Drivers and Impacts of the Record-Breaking 2023 Wildfire Season in Canada, Nature Communications, 15, 6764, https://doi.org/10.1038/s41467-024-51154-7, 2024.

Kasischke, E. S., O'Neill, K. P., French, N. H. F., and Bourgeau-Chavez, L. L.: Controls on Patterns of Biomass Burning in Alaskan Boreal Forests, p. 173–196, Springer, https://doi.org/10.1007/978-0-387-21629-4_10, 2000.

Kuntzemann, C. E., Whitman, E., Stralberg, D., Parisien, M.-A., Thompson, D. K., and Nielsen, S. E.: Peatlands promote fire refugia in boreal forests of northern Alberta, Canada, Ecosphere, 14, e4510, https://doi.org/10.1002/ecs2.4510, 2023.

Kurz, W. A., Apps, M., Banfield, E., and Stinson, G.: Forest carbon accounting at the operational scale, The Forestry Chronicle, 78, 672–679, https://doi.org/10.5558/tfc78672-5, 2002.

Letang, D. and de Groot, W.: Forest floor depths and fuel loads in upland Canadian forests, Canadian Journal of Forest Research, 42, 1551–1565, https://doi.org/10.1139/x2012-093, 2012.

Linn, R. R., Goodrick, S. L., Brambilla, S., Brown, M. J., Middleton, R. S., O'Brien, J. J., and Hiers, J. K.: QUIC-fire: A fast-running simulation tool for prescribed fire planning, Environmental Modelling and Software, 125, 104 616, https://doi.org/10.1016/j.envsoft.2019.104616, 2020.

McAlpine, R. S.: Testing the Effect of Fuel Consumption on Fire Spread Rate, International Journal of Wildland Fire, 5, 143–152, https://doi.org/10.1071/wf9950143, 1995.

McRae, D. J., Lynham, T. J., and Frech, R. J.: Understory prescribed burning in red pine and white pine, The Forestry Chronicle, 70, 395–401, https://doi.org/10.5558/tfc70395-4, 1994.

McRae, D. J., Stocks, B. J., Mason, J. A., Lynham, T. J., Blake, T. W., and Hanes, C. C.: Influence of ignition type on fire behavior in semi-mature jack pine., Information Report GLC-X-19, http://cfs.nrcan.gc.ca/publications?id=38237, 2017.

Melton, J. R., Arora, V. K., Wisernig-Cojoc, E., Seiler, C., Fortier, M., Chan, E., and Teckentrup, L.: CLASSIC v1.0: the open-source community successor to the Canadian Land Surface Scheme (CLASS) and the Canadian Terrestrial Ecosystem Model (CTEM) – Part 1: Model framework and site-level performance, Geoscientific Model Development, 13, 2825–2850, https://doi.org/https://doi.org/10.5194/gmd-13-2825-2020, 2020.

Michaletz, S. T. and Johnson, E. A.: A heat transfer model of crown scorch in forest fires, Canadian Journal of Forest Research, 36, 2839–2851, https://doi.org/10.1139/x06-158, publisher: NRC Research Press, 2006.

O'donnell, J. A., Harden, J. W., McGUIRE, A. D., Kanevskiy, M. Z., Jorgenson, M. T., and Xu, X.: The effect of fire and permafrost interactions on soil carbon accumulation in an upland black spruce ecosystem of interior Alaska: implications for post-thaw carbon loss, Global Change Biology, 17, 1461–1474, https://doi.org/10.1111/j.1365-2486.2010.02358.x, _eprint: https://onlinelibrary.wiley.com/doi/pdf/10.1111/j.1365-2486.2010.02358.x, 2011.

Parisien, M.-A., Barber, Q. E., Hirsch, K. G., Stockdale, C. A., Erni, S., Wang, X., Arseneault, D., and Parks, S. A.: Fire deficit increases wildfire risk for many communities in the Canadian boreal forest, Nature Communications, 11, 1–9, https://doi.org/10.1038/s41467-020-15961-y, 2020.

Parks, S. A., Parisien, M.-A., Miller, C., Holsinger, L. M., and Baggett, L. S.: Fine-scale spatial climate variation and drought mediate the likelihood of reburning, Ecological Applications, 28, 573–586, https://doi.org/10.1002/eap.1671, 2018.

Pérez-Izquierdo, L., Clemmensen, K. E., Strengbom, J., Nilsson, M.-C., and Lindahl, B.: Quantification of tree fine roots by real-time PCR, Plant and Soil, 440, 593–600, https://doi.org/10.1007/s11104-019-04096-9, 2019.

Simon, H., Beck, L., Bhave, P. V., Divita, F., Hsu, Y., Luecken, D., Mobley, J. D., Pouliot, G. A., Reff, A., Sarwar, G., and Strum, M.: The development and uses of EPA's SPECIATE database, Atmospheric Pollution Research, 1, 196–206, https://doi.org/10.5094/APR.2010.026, 2010.

Skakun, R., Castilla, G., Metsaranta, J., Whitman, E., Rodrigue, S., Little, J., Groenewegen, K., and Coyle, M.: Extending the National Burned Area Composite Time Series of Wildfires in Canada, Remote Sensing, 14, 3050, https://doi.org/10.3390/rs14133050, 2022.

Smyth, C., Xie, S., Zaborniak, T., Fellows, M., Phillips, C., and Kurz, W. A.: Development of a prototype modeling system to estimate the GHG mitigation potential of forest and wildfire management, MethodsX, p. 101985, https://doi.org/10.1016/j.mex.2022.101985, 2022.

Smyth, C., Fellows, M., Morken, S., and Magnan, M.: Development of national post-fire restoration system to assess net GHG impacts and salvage biomass availability, MethodsX, 13, 102 932, https://doi.org/10.1016/j.mex.2024.102932, 2024.

Stenzel, J. E., Bartowitz, K. J., Hartman, M. D., Lutz, J. A., Kolden, C. A., Smith, A. M. S., Law, B. E., Swanson, M. E., Larson, A. J., Parton, W. J., and et al.: Fixing a snag in carbon emissions estimates from wildfires, Global Change Biology, 25, 3985–3994, https://doi.org/10.1111/gcb.14716, 2019.

Stinson, G., Thandi, G., Aitkin, D., Bailey, C., Boyd, J., Colley, M., Fraser, C., Gelhorn, L., Groenewegen, K., Hogg, A., and et al.: A new approach for mapping forest management areas in Canada, The Forestry Chronicle, 95, 101–112, https://doi.org/10.5558/tfc2019-017, 2019.

Stocks, B. J., Mason, J. A., Todd, J. B., Bosch, E. M., Wotton, B. M., Amiro, B. D., Flannigan, M. D., Hirsch, K. G., Logan, K. A., Martell, D. L., and et al.: Large forest fires in Canada, 1959–1997, Journal of Geophysical Research: Atmospheres, p. FFR 5–12, https://doi.org/10.1029/2001JD000484, 2002.

Stocks, B. J., Alexander, M. E., Wotton, B. M., Stefner, C. N., Flannigan, M. D., Taylor, S. W., Lavoie, N., Mason, J. A., Hartley, G. R., Maffey, M. E., and et al.: Crown fire behaviour in a northern jack pine-black spruce forest, Canadian Journal of Forest Research, 34, 1548–1560, https://doi.org/10.1139/x04-054, 2004.

Strong, W. L. and La Roi, G. H.: Root density-soil relationships in selected boreal forests of central Alberta, Canada, Forest Ecology and Management, 12, 233–251, https://doi.org/10.1016/0378-1127(85)90093-3, 1985.

Talucci, A. C. and Krawchuk, M. A.: Dead forests burning: the influence of beetle outbreaks on fire severity and legacy structure in sub-boreal forests, Ecosphere, 10, e02 744, https://doi.org/10.1002/ecs2.2744, 2019.

Thompson, D. K., Simpson, B. N., Whitman, E., Barber, Q. E., and Parisien, M.-A.: Peatland Hydrological Dynamics as A Driver of Landscape Connectivity and Fire Activity in the Boreal Plain of Canada, Forests, 10, 534, https://doi.org/10.3390/f10070534, 2019.

Trofymow, J. A., Moore, T. R., Titus, B., Prescott, C., Morrison, I., Siltanen, M., Smith, S., Fyles, J., Wein, R., Camiré, C., Duschene, L., Kozak, L., Kranabetter, M., and Visser, S.: Rates of litter decomposition over 6 years in Canadian forests: influence of litter quality and climate, Canadian Journal of Forest Research, 32, 789–804, https://doi.org/10.1139/x01-117, publisher: NRC Research Press, 2002.

Turetsky, M. R., Amiro, B. D., Bosch, E., and Bhatti, J. S.: Historical burn area in western Canadian peatlands and its relationship to fire weather indices, Global Biogeochemical Cycles, 18, https://doi.org/10.1029/2004GB002222, 2004.

Walker, X. J., Baltzer, J. L., Bourgeau-Chavez, L. L., Day, N. J., De Groot, W., Dieleman, C., Hoy, E. E., Johnstone, J. F., Kane, E. S., Parisien, M. A., and et al.: ABoVE: Synthesis of Burned and Unburned Forest Site Data, AK and Canada, 1983-2016, ORNL DAAC, https://doi.org/10.3334/ORNLDAAC/1744, 2020.

White, J. C., Wulder, M. A., Hermosilla, T., Coops, N. C., and Hobart, G. W.: A nationwide annual characterization of 25years of forest disturbance and recovery for Canada using Landsat time series, Remote Sensing of Environment, 194, 303–321, https://doi.org/10.1016/j.rse.2017.03.035, 2017.

Whitman, E., Parisien, M.-A., Thompson, D. K., Hall, R. J., Skakun, R. S., and Flannigan, M. D.: Variability and drivers of burn severity in the northwestern Canadian boreal forest, Ecosphere, 9, e02 128, https://doi.org/10.1002/ecs2.2128, 2018.

Whitman, E., Parisien, M.-A., Holsinger, L. M., Park, J., and Parks, S. A.: A method for creating a burn severity atlas: an example from Alberta, Canada, International Journal of Wildland Fire, https://doi.org/10.1071/WF19177, 2020.

Whitman, E., Barber, Q. E., Jain, P., Parks, S. A., Guindon, L., Thompson, D. K., and Parisien, M.-A.: A modest increase in fire weather overcomes resistance to fire spread in recently burned boreal forests, Global Change Biology, 30, e17 363, https://doi.org/10.1111/gcb.17363, 2024.